Diagnostic instrumentation for plasma physics experiments at the APPA cave

Technical Design Report

P. Neumayer, O. Rosmej, J. Jacoby, A. Blazevic, M. Roth, A. Ulrich, C. Spielmann
for the HEDgeHOB and WDM collaboration

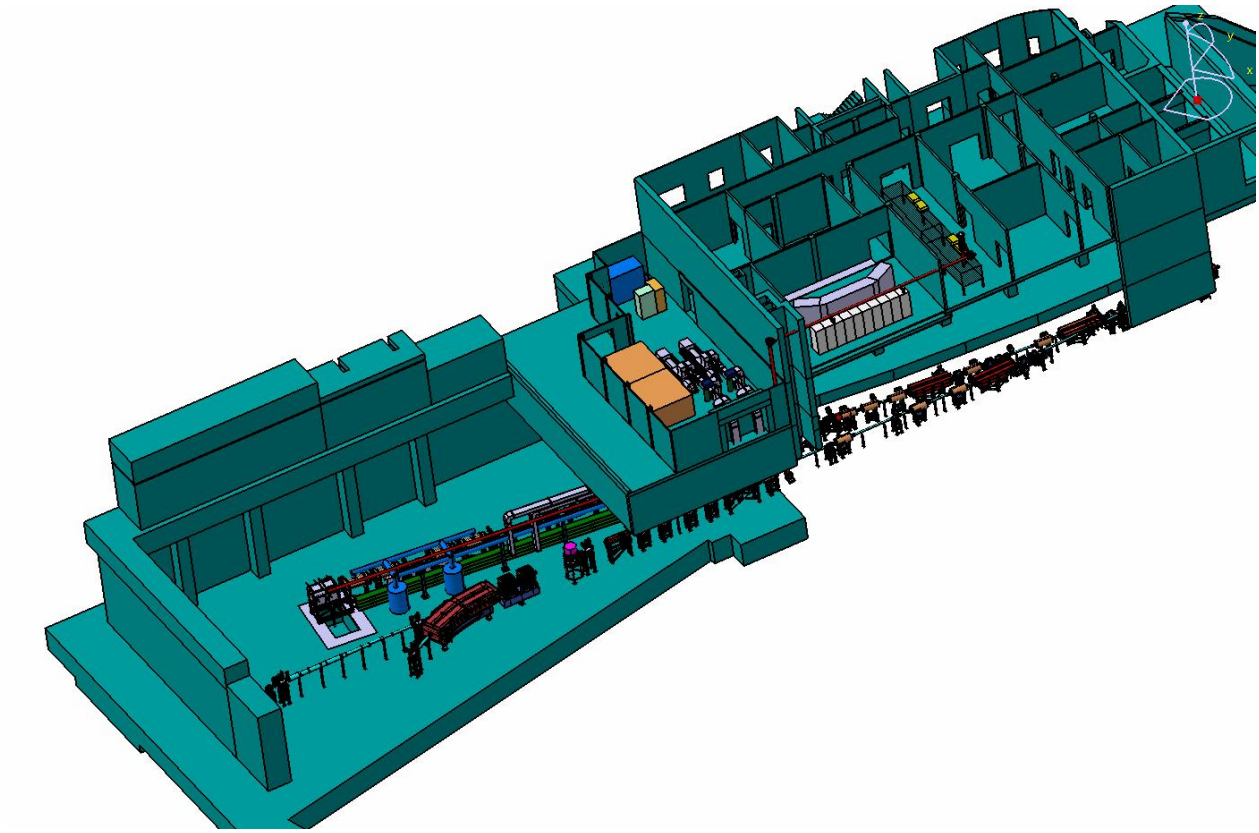

Contents

Introduction: High Energy Density Science at FAIR

Matter at high energy density occurs widely in the universe, making up most of the matter condensed in compact astrophysical objects such as planets, brown dwarfs and stars. Modeling of such objects with the goal of revealing their interior structure and composition, and learning about the formation and evolution requires accurate knowledge of material properties, such as the equation-of-state, phase boundaries, optical and electrical properties. Typical conditions found in giant planets are pressures exceeding 1Mbar and reaching up to Gbar, densities around solid density up several times solid, and temperatures of order eV. Matter at these conditions is often also referred to as warm-dense matter (WDM). Modeling of matter at warm-dense conditions remains a grand challenge. The interaction potential between the ions is comparable to the thermal energy, thus the system is strongly coupled, and expansion techniques that treat the interaction as a small perturbation are no longer applicable. Also, the de-Broglie wavelength of the electrons is comparable to the interparticle distance, so quantum effects have to be taken into account. Highly computing intensive ab-initio methods are becoming the state-of-the-art tool to predict matter properties. These calculations are used to generate the EOS over the entire parameter range inside giant planets [Net2008]. They predict phase boundaries such as melting lines [Knu2008], metallization or new high-pressure solid phases [Wil2013], opacities [Vin2009], conductivities, H-He demixing [Lor2011] which are all of high relevance for understanding the planets found within our solar system as well as the thousands of exo-planets currently being discovered. Besides the fundamental interest in the complex behavior of strongly-coupled, partly degenerate many-body systems, and its application for predicting planetary interiors, understanding and controlling matter at extreme conditions also is of relevance for technological applications, for example when matter is exposed to large particle fluxes as in the first wall of a fusion reactor, accelerator beam dumps, laser-matter interaction experiments, i.e. whenever transformation from solid to plasma occurs.

Experimental investigation of high energy density (HED) matter has become a fast growing field with the advent of high power facilities, such as high-power laser and Z-pinch-systems. These can deposit a significant amount of energy to heat and/or compress matter on a time-scale short enough to dynamically reach HED conditions. A prerequisite for accurate, quantitative measurements of material properties are well-controlled schemes to generate a sizable amount of HED matter at equilibrium conditions with small gradients

Unprecedented ion beams capabilities at FAIR will offer world-wide unique opportunities for dense plasma research. Intense pulses of uranium ions focused to millimeter spotsizes deposit energy densities of order 10kJ/g. Time-scales of order 100ns ensure equilibrium conditions, while ion beam stopping ranges of order cm allow for homogenous energy deposition in large samples with small gradients. Two large collaborations, the HEDgeHOB (High-Energy Density generated by Heavy Ion Beams) and the WDM (Warm Dense Matter) collaboration, have put forward proposals to exploit these unique opportunities [HED2005, WDM2006]. A variety of schemes have been suggested to employ FAIR heavy ion beams to create samples of matter at high energy density conditions. They can be roughly grouped into two categories.

Heavy ion heating

In the first scheme the ion beam directly heats the sample under investigation. At energy deposition up to 10kJ/g results in Mbar pressures and eV temperatures. Typically, the target will undergo expansion

while being heated (HIHEX: Heavy Ion Heating and Expansion). This way high-entropy plasma states over a wide parameter range in the temperature/density phase space can be accessed [Tah2005]. The free expansion of the heated sample can be contained by surrounding the target with a strong wall of a different material, transparent either in the visible (i.e. LiF or Sapphire window) or in the x-ray regime (e.g. BN or B_4C). Specific schemes have been explored where the expansion is completely suppressed by surrounding the sample material with a tamper which will be heated by the ion beams as well, thus generating an inwards pressure (Dynamic Confinement, [Koz2003]). Heating of thin foils on the other hand has been suggested to result in an isothermally heated sample providing an interesting testbed for opacity measurements in the VUV and soft x-ray spectral region cite [Tau2009].

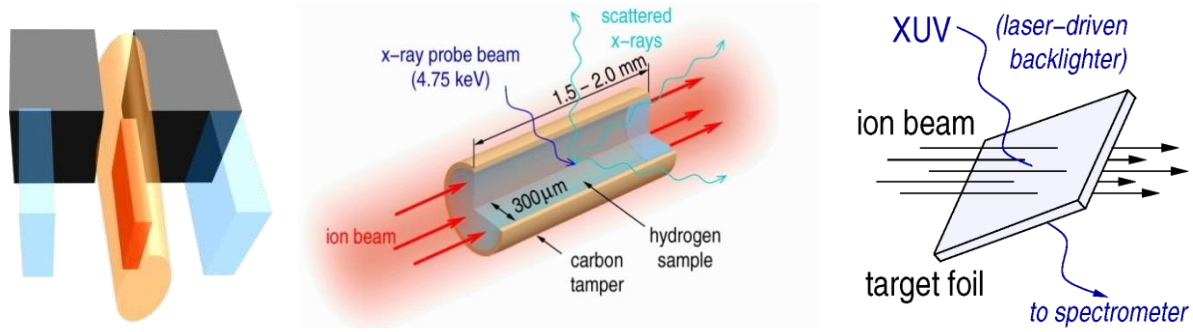

Figure 1: Various schemes proposed for heavy ion heating: (left) HIHEX scheme with a high-Z target, expanding between two sapphire windows, (middle) dynamic confinement, (right) thin foil heating for opacity studies

LAPLAS

In the LAPLAS (LAboratory PLAnetary Science) scheme a cylindrical sample is surrounded by a high-Z tamper. A so-called wobbler module induces a fast rotation of the ion beam in the focal plane, effectively generating a ring-shaped focus, thus allowing energy deposition into the tamper without heating the sample material in the center (Fig. 2). Expansion of the heated tamper will result in a cylindrically symmetric inwards movement and a near-isentropic compression of the sample material, generating matter at conditions comparable to the interior of planets. For example, it has been shown that with this scheme super-ionic water can be generated which is expected to be prevalent inside the ice giants Uranus and Neptune [Tah2010]. More recent simulations indicate that iron at earth core conditions and even those expected in “super-earths” can be produced with the LAPLAS scheme [Tah2014].

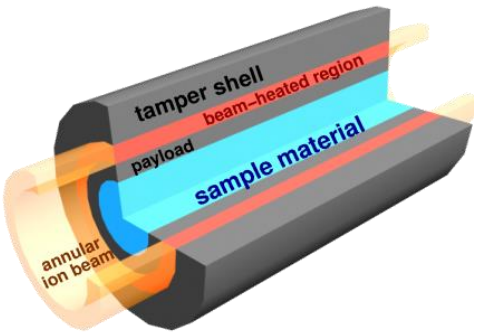

Figure 2: LAPLAS scheme. The ring-shaped heavy-ion beam heats the cylindrical tamper, inwards expansion results in near-isentropic compression of the sample material.

Dense matter backlighting capabilities

High-energy high-intensity laser

Active backlighting with highly penetrating laser accelerated particles or x-ray radiation will be one of the primary diagnostic tools to access plasma parameters and structural information from inside the dense samples. Intense x-ray pulses with sufficient brightness to probe the short-lived samples can be obtained from high-energy laser-driven plasmas. Probing the millimetre-size high-Z targets foreseen in the plasma physics program will require highly penetrating hard (>100 keV) x-ray sources, typically obtained from laser systems delivering focused intensities in excess of 10^{18}W/cm^2 [Par2008,Tom2011]. As an example, Figure 3 shows an example of a lead target, driven by FAIR heavy ion beams in the HIHEX scheme [Tah2005]. Calculated point projection radiographs, assuming a hard x-ray source from a thin high-Z foil driven by a kJ/ps-type laser, suggest spatial resolution of order 10µm and density resolution of a few percent can be achieved. Other secondary radiation sources with large diagnostic potential for dense samples include laser-accelerated protons [Cow2004], neutrons [Rot2013], and electrons [Wil2013]. A first proposal for such a laser has been made in the initial version of FAIR, and a space located between the APPA cave and the High-Energy Storage Ring has been reserved for a high-energy petawatt laser.

As first step in the technological development of this laser system, and more importantly to provide initial backlighting and other laser-based diagnostic capabilities, a smaller scale high-energy laser has been applied for. Expected parameters of this laser will be laser pulses of energy 100J at a wavelength of 527nm, with pulse durations between 100ps and 10ns. Reaching focused intensities in the range of 10^{12}… 10^{16} W/cm^2 this system will allow driving intense laser-plasma sources for backlighting from XUV to ~10keV continuous and line-sources. These sources will already enable a wide range of x-ray backlighting diagnostic schemes on lower-Z targets, such as keV-radiography using pinhole imaging, VUV-opacity measurements, x-ray near-edge absorption structure, x-ray diffraction and x-ray scattering.

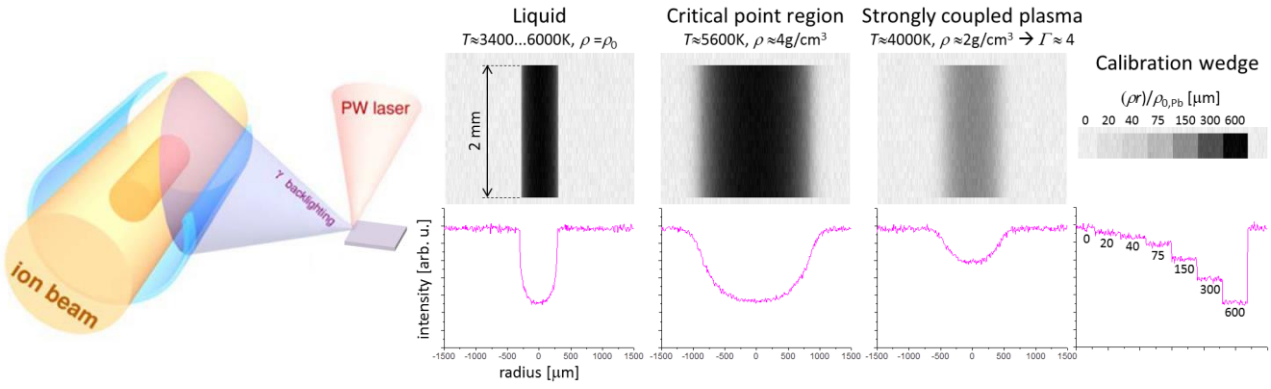

Figure 3: Schematic of a HIHEX experiment, employing point-projection hard x-ray backlighting radiography (left). Simulated radiographs of various plasma states realized by heavy-ion heating of a cylindrical lead target (right).

Proton radiography setup

Besides using FAIR heavy ion beams to generate HED matter samples, the ion beam can also serve as a diagnostic for dense matter. Protons with 4.5GeV energy delivered by FAIR have large ranges in solid density matter, providing a probe for high rho-r samples. A combination of magnetic lenses transforms nuclear scattering into attenuation and provides imaging and magnification. This way the target mass density distribution can be imaged. With several 10^{10} protons per pulse, spatial resolution of order 10μm as well as temporal resolution below 10ns can be expected. PRIOR will thus provide an accurate space- and time-resolved density measurement for experiments with externally driven (lasers, pulsed power, high explosives, etc.) samples.

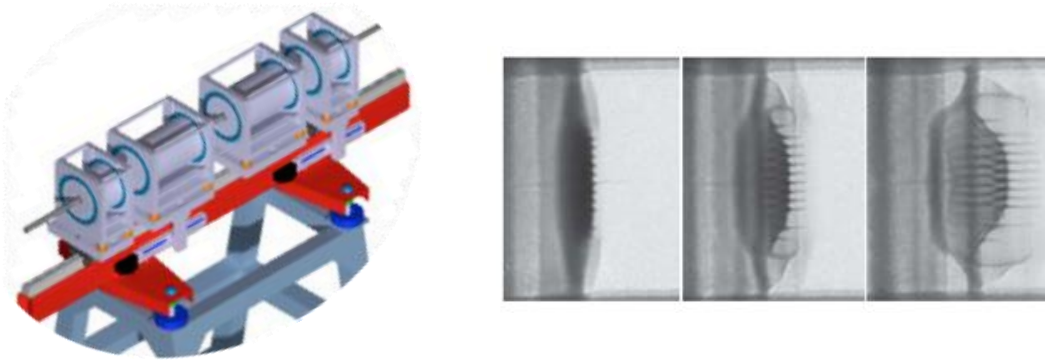

Figure 4: In the prototype proton microscope PRIOR at GSI (left), Proton radiograph of a growing Richtmyer-Meshkov instability (right, courtesy of LANL).

Diagnostic requirements for plasma physics experiments at FAIR

Fielding the experiments outlined above will require diagnostics well matched to the particularities of relativistic ion-driven plasmas. While part of this equipment can be readily purchased, other detectors need certain development. The goal of this document is to motivate what is considered the basic and indispensable equipment to enable first plasma physics experiments, and to explain specifications and design considerations. In order to provide a certain structure we have divided the diagnostic equipment somewhat artificially into three categories, diagnostics based on *optical light*, *x-ray radiation* (including the XUV and the hard x-ray regime), and *particles* (protons, neutrons and electrons).

Besides the requirements specific to each type of probe and the experimental scheme in which it is used a few general requirements can be sketched, given the properties of the ion pulses and the particular scenario of heating with relativistic ion beams at highest intensities. These will be given in the following.

The minimum ion focus diameter is of order 1mm, with approximately Gaussian distribution. In order to resolve transverse spatial gradients, a *spatial resolution* of order 10μm at the target should be sufficient. This resolution goal is also in compliance with proposed Richtmyer–Meshkov instability growth studies [Tah2011], where the relevant scale is not given by the ion beam size, but rather by the perturbation wavelength. The relevant *temporal scale* can be assessed by comparing the spatial scale with typical sound or shock velocities. At 5-10km/s, the spatial scale of 10μm translates into a time scale

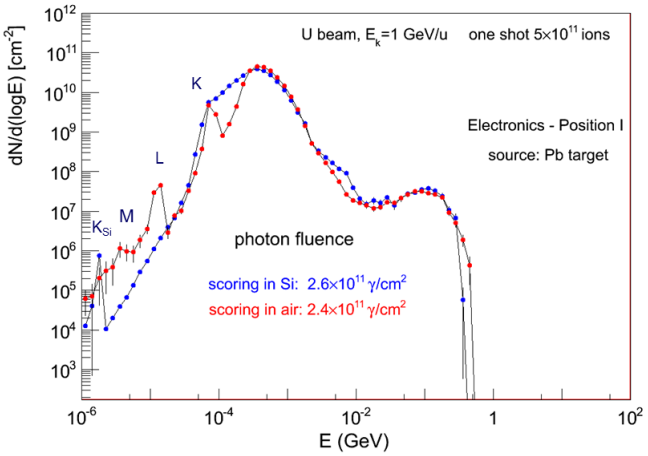

Figure 5: X-ray flux emitted by a lead target that is heated by an intense heavy ion pulse.

of 1-2ns. This is well below the expected ion pulse duration (50-100ns), thus also sufficient to probe the target temporal evolution during the heating pulse.

Extensive Monte-Carlo simulations have been carried out in order to determine the amount of radiation produced during the interaction of the relativistic heavy ion pulse with the target. Especially when ion beams at the highest anticipated intensities interact with large (several mm) targets a significant amount of x-rays, high-energy hadrons and neutrons will be generated. This has several implications. The background signal generated by the secondary radiation might in most cases severely limit the achievable signal-to-noise ratio, or even render a measurement altogether impossible. For example, Figure 5 shows the x-ray flux emitted from a lead target, irradiated by $5x10^{11}$ uranium ions at 1GeV/u, at a distance of 10cm from the target. It can be seen that large amounts of x-ray radiation is emitted, both line-radiation from inner-shell transitions as well as continuous bremsstrahlung emission, ranging from keV to nearly GeV photon energies. This radiation will cause a significant background level, most likely both in dedicated x-ray diagnostics, as well as other types of detectors (charged particle, visible). We therefore expect that *temporal gating* of the data acquisition will be a crucial requirement for most diagnostics.

Secondary radiation also poses a severe risk for radiation damage to data acquisition electronics. Experience at GSI's former plasma physics cave has shown that heavy shielding and location of detector electronics upstream of the ion beam are mandatory to avoid degradation or loss of equipment. Figure 6 shows the calculated dose distribution in the APPA cave, accumulated over 1 year of beamtime operation. For this calculation the worst scenario (in terms of production of secondary radiation) has been considered, i.e. a total of 5760 shots (1 shot per 10 minutes for 4 x 10 days per year) at $5x10^{11}$ ions per shot onto a large (length 27 mm, diameter 7 mm) Pb-target (most likely the use of such extremely massive targets and high fluences will be strongly restricted). Close to the target and in ion beam forward direction, the accumulated dose reaches values of several hundred Gy which would destroy sensitive electronics. Similarly, high neutron fluences (up to 10^{15} MeV-equivalent neutrons per cm^2) and high-energy hadrons (up to $10^{12}/cm^2$) will rapidly cause severe degradation of electronics equipment. However, it can also be seen, that radiation levels significantly drop with increased distance from the target chamber over several orders of magnitude. In particular, at a few meters upstream the dose falls below 10 Gy (Figure 6), the neutron fluence (1 MeV-eq) below $10^{12}/cm^2$, and the fluence of high-energy

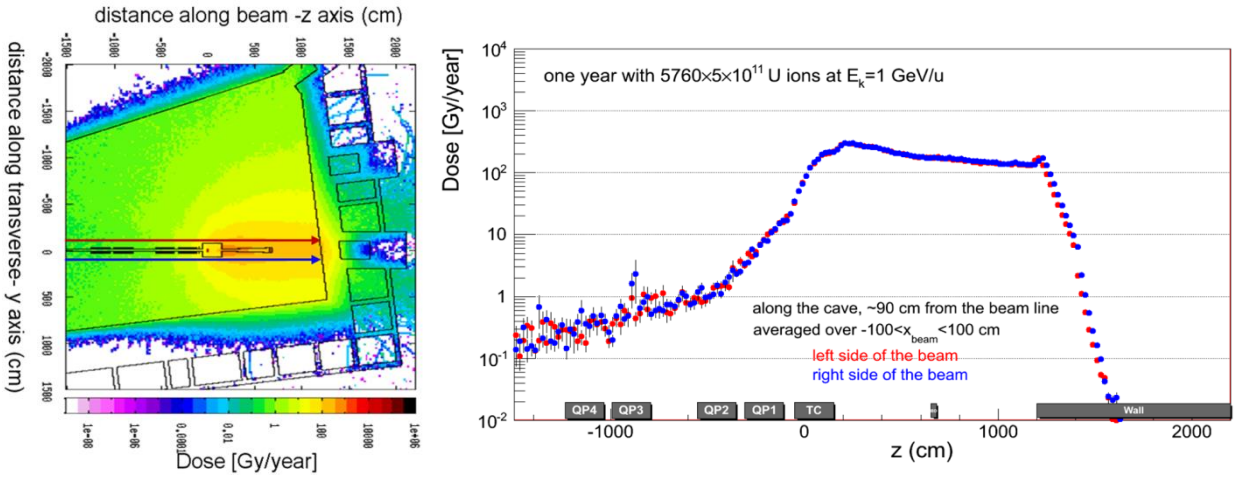

Figure 6: Dose distribution in the APPA cave accumulated over 1 year of operation (left). Upstream of the target chamber the dose is significantly reduced (right).

hadrons below 10^9/cm^2 (not shown here). These levels are considered to cause no significant equipment degradation.

Consequently, another important design criterion for diagnostic equipment in the APPA cave will be that data acquisition electronics should whenever possible be *located far from the target*. This conflicts with the usual need for a sizable detection solid angle to collect sufficient signal for high-quality data. A promising approach to this is the conversion of diagnostic radiation to scintillation light and subsequent transport via high-NA optical imaging or coherent fiber bundles for digitization far from the interaction. This separation will also allow significant additional shielding of the electronics and enclosures will help mitigate possible EMP (electro-magnetic pulse) issues expected when a high-intensity laser will become available.

Furthermore, the calculations show that nuclear reactions will lead to considerable activation of the remaining target debris, target chamber, and the material close-by. Figure 7 shows the calculated

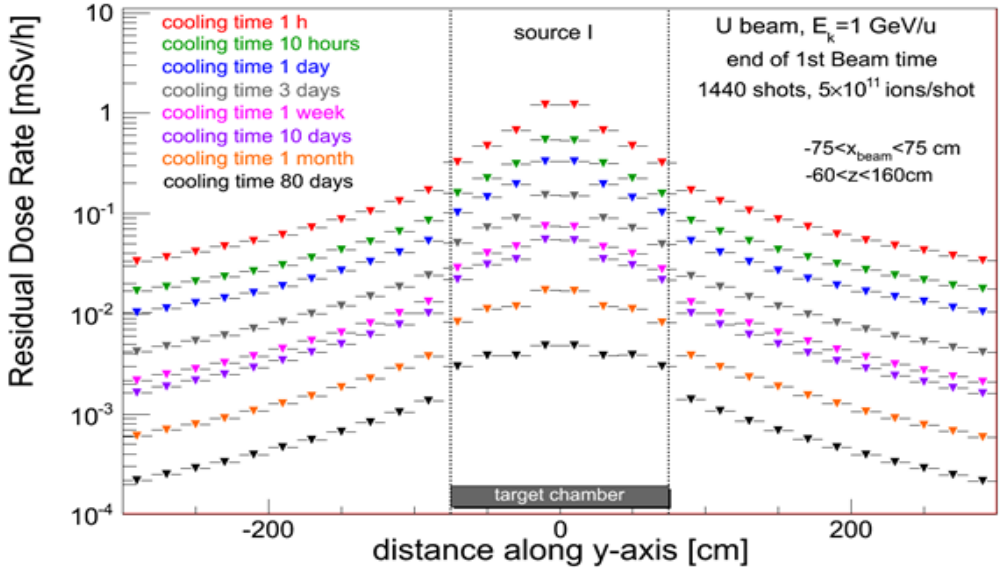

Figure 7: Residual dose inside and around the target chamber, at the end of a high-intensity U beamtime.

residual dose after a beamtime using $5x10^{11}$ uranium ions per pulse. Right after the beamtime the dose close to the target chamber only allows short activities, and several days of decay time might be required until the residual dose has decreased to a level that permits human activity inside the target chamber. Therefore, in particular in experiments involving large high-Z targets and highest ion beam intensities detection schemes that require physical removal of the detector to access the experimental data (e.g. film, image plate, RCF) are strongly discouraged. Rather, detection systems should allow *electronic readout* as well as *remote operation*.

1. Optical diagnostics

Optical target characterization

Although optical radiation (ranging from the near-infrared to the ultra-violet spectral range) does not penetrate through dense matter, optical diagnostics will play a major role in plasma physics experiments conducted at FAIR. Target temperatures in HIHEX-experiments [Tah2005] up to several eV are expected. Considering spectrum close to the Planckian one, the maximum of the plasma self-radiation will cover IR, optical and UV-regions of EM-spectrum.

Due to volumetric heating by the heavy ion beam a nearly homogeneous distribution of plasma parameters is expected and measurements of the target surface color temperature using narrow band filter set can be used to deduce the plasma temperature in the target center. Emission in the optical

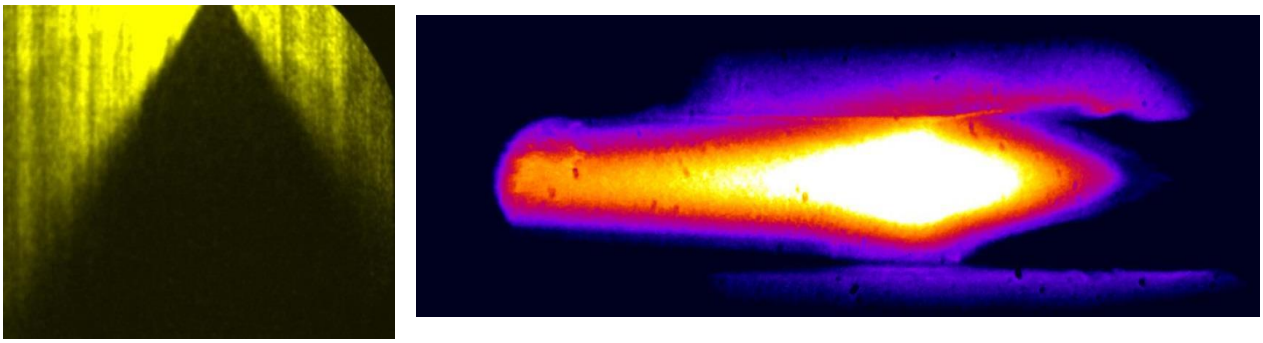

Figure 8: Streaked optical shadowgraph of an expanding heavy-ion heated target (left), and gated image of the heated target optical emission (right).

from the target surface can also yield information on the hydrodynamic process inside the target, providing strong boundary conditions for target simulations as well as benchmarking the hydrodynamic performance of the target. The abrupt increase in emission is a clear indication for shock breakout and provides the shock velocity. In combination with an external probe laser, reflectivity measurements can be performed, directly accessing the target optical properties, which are linked to the electronic conductivity. Interferometric surface velocity measurements (VISAR, e.g. [Cel2004]) provide particle velocity and in combination with shock velocity measurement the shock pressure. For low-density expanding plasmas as those from thin ion-heated foils the density distribution can also be probed by optical interferometric methods.

Ion beam diagnostics

Besides these extremely important applications for target performance and characterization, measurement of optical radiation will be crucial to the assessment of the ion beam focusing in the target chamber. Very intense beams as planned for FAIR lead to the problem that regular beam diagnostic tools such as grids can no longer be used to measure the beam profiles because they would be destroyed by energy deposition by the beam. Optical diagnostics is considered as an alternative, while solid state scintillators cannot be used for the same reasons. The concept is to fill parts of the beam-line or the target region with gas. Particle beam excitation of the gas leads to light emission which is an indication for the presence and the shape of the beam. However, several aspects concerning the light emission process have to be considered for a practical application of the concept.

Particle beam induced light emission from gases is a rather complex field of research [Ulr2012] because of the various parameters which are involved such as the gas composition, the gas density, as well as the type of light-producing particle and its energy. A key issue for the case of ion beams is that both the ion beam projectiles and secondary electrons (or partly also secondary ions or nuclear reaction products) contribute to the excitation and ionization of the gas. Briefly, a glowing core directly excited by the beam projectiles and a halo excited by the secondary particles has to be expected. Gas density and the type of excitation processes will influence the shape and radius of these regions. A proposal for a basic concept which has been brought forward to identify the actual shape of the beam is the following: Formation of multiple ionized atoms in excited states have high cross-sections in single heavy ion collisions [Coc1979]. The same processes should on the other hand be negligible for secondary electrons. Therefore it is planned to perform a detailed study to identify appropriate spectral lines originating from multiple ionized species with the goal to find conditions where the light emission is produced as locally as possible within the flux of the actual beam particles. The concept has already been described and partially tested in [Var2009, Ulr2012], so the risk for this diagnostic to not fulfill the requirements is fairly low. Nevertheless, alternative schemes to determine the ion energy deposition in the target by x-ray imaging are being explored (see Chapter 2 on X-ray diagnostics).

Gated cameras allow 2-dimensional imaging at a particular time, given by the gate, and accumulate image information during a well-defined time window (exposure time). A sequence of images spread over time can be realized either by using several framing cameras, triggered one after the other, or by multi-framing devices. Gated cameras for optical target diagnostics will be required for optical emission measurements from the ion-heated targets, e.g. to perform pyrometry to assess the target temperature, and more generally, to observe the overall target evolution and experiment performance. Therefore, we foresee a total of 8 fast-gated imaging channels.

By contrast, streak cameras provide a continuous measurement over time by temporally streaking the optical information over the detector plane. Consequently, only one dimension is available for imaging. In a VISAR setup, streak cameras are used to give a continuous temporal record of the fringe-shifts of a velocity interferometer, providing the target surface velocity, while imaging a line across the target [Cel2004]. In order to avoid fringe shift ambiguities, two individual channels (i.e. interferometer + streak camera) with different velocity sensitivity are necessary. In addition, streak cameras will be required to provide continuous temporal information for determination of shock break-out times.

2. X-ray diagnostics

Energetic photons are one of the prime diagnostic probes for dense plasmas as those produced with intense heavy ion beams at FAIR. For optical light (photon energies of eV) the critical density beyond which electromagnetic radiation cannot penetrate further of order 10^{21}electrons/cm^3 and thus far below typical solid densities. By contrast, the critical density for x-rays is well above the electron density in solids, and thus can reveal information from within the dense plasmas under investigation.

Imaging of the absorption (photo-ionization, Compton scattering) directly yields the target density distribution. As photons interact with the electrons in the system, x-ray emission, absorption and scattering techniques give access to the charge state distribution and electron excitation spectrum providing a stringent benchmark for dense matter calculations. In addition, as the wavelength of x-ray radiation is comparable to the interparticle distances, diffraction can give information on the microscopic structure and order of the system (similar to well-established solid state crystallography techniques).

X-ray imaging detectors

Detection of x-rays with 2-dimensional spatial resolution is a prerequisite for most of the x-ray diagnostic schemes. Radiographic images are obtained by projecting x-rays of a backlighter source transmitted through the target (either by point-projection of imaged by a pinhole aperture) onto a 2D-detector (see e.g. Figure 3). X-ray diffraction techniques require a 2D-detector to record the diffraction pattern. In spectroscopic schemes, energy resolution is typically realized by wavelength-dispersive methods, where diffraction off a grating or crystal maps the photon energy onto a spatial coordinate. Using curved crystals simultaneous spatial resolution in one direction can be achieved.

In typical high energy density experiments the target is destroyed and has to be replaced after each shot and the usual diagnostic approach is to acquire a complete “image” within a single-shot. This means that single-photon detection relying on the accumulation of thousands of events is not applicable. Instead, integrating detectors with a high dynamic range (>1000) are required. Resolution requirements depend on the application. Radiography schemes often easily allow for magnification of order 10…20x, thus a detector pixel resolution of order 100-200 micrometers is sufficient to provide 10μm resolution at the target. X-ray diffraction spots typically are of the same size as the probed region, i.e. also here a detector resolution of 100μm will be sufficient. Imaging crystal spectrometers on the other hand often cannot realize too large magnification, if efficiency and spectral range have to fulfill certain requirements. Here, the desired resolution depends on the specific experiment. When imaging along the ion beam propagation in most cases a resolution of 100μm will be sufficient, due to the long stopping range of the relativistic ions. Imaging in a direction transverse to the ion beam (spot diameter 1mm) might in some cases allow for a resolution of only 100μm. A spatial resolution of the imaging detector would therefore in most cases limit the achievable spectral resolution.

Imaging plates

Imaging plate detectors are widely used in medical imaging applications involving x-rays with energies of up to 100 keV. The imaging plate is doped with a photostimulable phosphor which is excited to a metastable state upon deposition of energy by ionizing radiation, e.g. by x-ray photons. The stored information can later be retrieved by scanning the image plate with a laser scanner which de-excites the phosphor, resulting in emission of fluorescence light.

Imaging plates are highly efficient detectors for photon energies ranging from <1keV to many 10's of keV. Typically resolution is limited to approx. 50-100µm and the dynamic range has been shown to be as large as 10^5. Imaging plates are very versatile and robust detectors. Sizes up to 0.5m are available, and the plate can be cut to almost any desired size and shape and even be bent, allowing use even in complicated diagnostic arrangements with limited space. Due to the off-line readout image plates are insensitive to EMP. All these features make imaging plates an almost ideal detector for x-rays over wide energy range (and also for other ionizing radiation, e.g. charged particles). Consequently, they have become a standard diagnostic in almost any experiment involving intense-laser plasma interaction. We therefore expect, at least in the initial phase of plasma physics experiments at the APPA cave, that imaging plates will play an important role as a well-understood, versatile and robust x-ray imaging detector. We therefore regard it as important to provide a standard image plate scanner, eraser and an initial set of imaging plates. Exchange of image plate detectors without venting the target chamber could be facilitated by load-lock systems that are currently under consideration.

X-ray CCD detectors

In a Charge-Coupled-Device (CCD) an incident photon is absorbed within the silicon of the detector chip, resulting in the production of the electron-hole pairs. The amount of charges created is digitized by an AD-converter and the digital image is available within fractions of a second, allowing for high repetition rate operation. Imaging cameras based on the CCD-scheme are easy-to-use versatile devices with a wide range of applications. The dynamic range is determined by the full-well-capacity, which depends on the pixel size. For 13µm pixel size, a dynamic of 10^4 is typically achieved. Electronic noise can by almost eliminated by Peltier-cooling of the detector to -20…-50°C. X-ray CCD detectors with back-thinned silicon chips feature high quantum efficiency at photon energies from 10eV to >10keV, and have been used for photon energies as high as 22keV. For even higher photon energies, the quantum efficiency drops significantly due to the low absorption probability in the detector.

Diagnostic use of an x-ray CCD camera for plasma physics experiment will be for high-resolution detection in the keV range. The camera can be used as detector for crystal spectrometers (x-ray scattering, absorption spectroscopy, XANES,…), monochromatic imaging, x-ray radiography using keV thermal plasma sources and pinhole or grazing-incidence reflection imaging, and even as a stand-alone single-photon counting spectrometer. The camera will also be indispensable for VUV- and XUV transmission measurements.

The use of the camera is however limited to experimental setups, where the camera can be placed in directions where secondary radiation from the heavy-ion heated target or the laser-driven plasma is not too severe, and can be sufficiently well shielded to not compromise the data or damage the detector. In a proof-of-principle experiment at the HHT experimental area behind the SIS at GSI, we have used this detector for XUV absorption measurements. Locating the camera upstream of the heavy ion beam and installation of baffles to limit the amount of secondary electrons

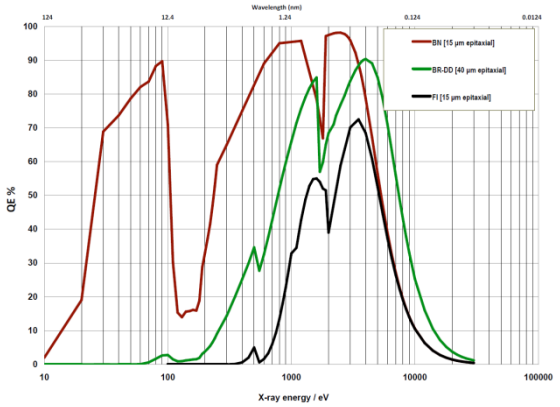

Figure 9: Quantum efficiency of various types of CCD detectors (red: back-thinned).

reaching the camera allowed recording VUV-spectra with acceptable background level.

Other limitations of the use of x-ray CCD cameras are experiments involving relativistic laser-matter interaction, which is anticipated when PW-class laser pulses will become available at the APPA-cave. In these experiments strong electromagnetic pulses are generated which often result in failures of the on-board electronics or read-out computer, and potentially even permanently destroying the detector. For these applications, either storing the image for readout after the experiment (imaging plate, see previous section), or conversion of x-rays to visible light, image transport and remote digitization are promising approaches for x-ray detection in high EMP and high-radiation environments.

Scintillator based imaging

X-ray detection by imaging plates requires physical removal of the plate from the experiment for off-line readout of the data. This strongly limits the available repetition rate of the experiment, as typically the detectors are fielded inside the target chamber (to provide proximity to the source, and to avoid absorption in air), and detector replacement requires venting and pump-down. In addition, short-lived activation of the target chamber will prohibit access to the experiment and removal of components until the activity has decayed to an acceptable level. Finally, for photon energies beyond 100keV the detection quantum efficiency of imaging plates decreases significantly due to the drop in absorption probability given by the rather thin low-Z sensitive layer (see Figure 10).

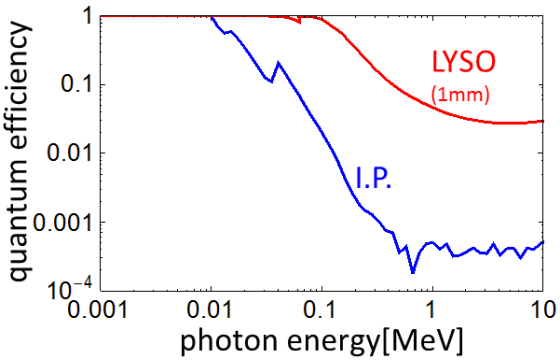

Figure 10: Quantum efficiencies of imaging plate (I.P.) and scintillation crystal.

Our approach to realize high quantum efficiency (QE) at MeV photon energies, full electronic readout for high repetition rate data acquisition and remote operation is to combine high-Z heavy scintillating crystals with highly-efficient fiber-optic image-relay and electronic readout of the optical light by visible CCD-camera. High-Z heavy crystal scintillators provide efficient absorption for energetic photons. Figure 10 shows the quantum efficiency of a 1mm thick LYSO (Lutetium Yttrium Orthosilicate) crystal, compared to that of an image plate. At photon energies above 100keV which will be required for

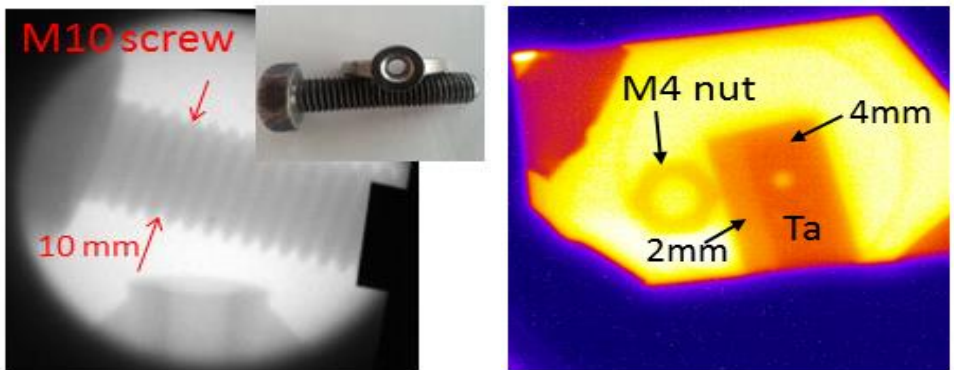

Figure 11: X-ray radiographic images obtained by the scintillator-based hard x-ray imager prototype, using bremsstrahlung produced by 6.5MeV electrons from the TU Darmstadt linear accelerator (left) and from a high-Z foil target irradiated with 100J/5ps laser pulses at the PHELIX facility (right).

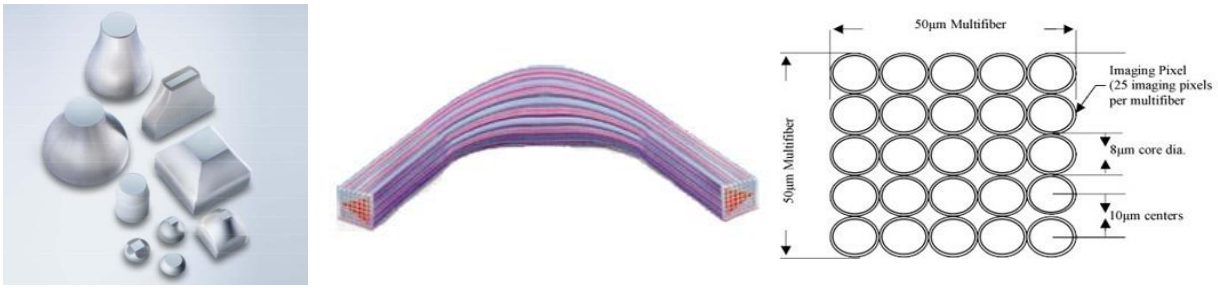

Figure 12: Fiber tapers for a variety of image formats (left) and coherent wound fiber bundles for image transport with 10 µm resolution.

penetrating large rho-r high-Z targets that are envisaged in the experiments proposed by HEDgeHOB, the scintillation crystal can easily exceed the image plate QE by 1-2 orders of magnitude. First radiography tests of these scintillators in combination with high numerical aperture imaging of the scintillation light onto an optical CCD camera have shown the potential of this approach (Figure 11).

We expect that digitization of the scintillation light has to be performed remotely to avoid exposure of the sensitive electronics to the harsh radiation background. Therefore, the scintillation light needs to be transported with highest possible efficiency over several meters to the camera location.

This is accomplished by demagnification of the scintillation screen by fiber optic tapers and subsequent image transport by fiber bundles (examples see Figure 12). Fiber tapers come in many different sizes, formats, and demagnification ratios. The Wound Fiber Optic Image Bundles consist of an array of optical fibers with distances of 10µm, allowing for resolutions of up to 50lp/mm with cross-sections as large as 8x10mm. Length up to almost 5m are available, which allows placing the camera at a large distance outside the target chamber with a big amount of shielding and only a minimal opening for the fiber bundle. Here the fiber bundle output is directly coupled to the CCD chip with another fiber taper. An image intensifier can be employed to boost the optical signal and to allow gating of the image to reduce ion beam generated background.

X-Ray and XUV spectroscopy

Besides spatially imaging the x-ray fluence transmitted through or diffracted by the target, the use of wavelength dispersive elements (crystals, gratings) allows for photon energy selection and resolution. Spherically bent crystals, tuned to an inner-shell transition that is excited by the heavy-ion beam crossing the target, can yield a quantitative image of the ion beam distribution inside the target not disturbed, as in the case of the optical image, by secondary electrons excitation of the target area across the ion tracks. This approach will be developed complementary to the imaging of specific optical transitions from highly excited atoms of a fill gas in the target chamber, as was discussed in the preceding chapter. Spherically bent crystals are also employed to achieve monochromatic imaging of a target for absolute plasma areal density measurement. Intense laser-driven plasma emitting strong Helium-alpha line radiation as a backlighter source allows monochromatic radiography (e.g. [Ben2008]), and the strong energy selectivity allows absolute areal density measurements, and strongly reduce the heavy-ion induced broadband background. Typical crystals used for these applications are quartz and mica, spherically curved at curvature radii of 100…300mm providing high spectral and spatial resolution [Fae1994, Ros2002]. For characteristic emission of high-Z targets photon energies above 20keV, transmission schemes, such as Cauchois type can be used [See2012].

In x-ray transmission spectroscopy, the transmission of an ideally broadband x-ray source through the sample is spectrally resolved. At higher temperatures, this can be employed as a sensitive charge state diagnostic [Saw2009]. For the low temperature plasmas expected in heavy-ion heated targets the technique of x-ray absorption near edge structure (XANES) has been found to be a powerful and sensitive diagnostic of both target temperature and density [Rec2009]. It has been applied to accurately characterize both shock and laser-proton heated samples [Ben2011, Man2010], and recent calculations suggest it can be applied to iron at earth core conditions [Maz2014]. XANES requires high-resolution crystal spectrometers, using e.g. Si or Ge crystals in the spectral range above 2.5keV, or potassium hydrogen phthalate (KAP) below 2keV.

Spectrally resolving x-rays scattered by the target accesses the electron excitation spectrum. Usually the elastic and inelastic scattering features, coming from tightly bound and free electrons, respectively, can be distinguished. The scattering strength of the elastic feature is closely connected with the ion-ion structure factor and thus reflects the microscopic order of the ionic sub-system. It has been successfully used in laser-driven experiments to assess target heating [Kri2008] and melting [Pel2010]. On the other hand, spectrally resolved measurements of the inelastic scattering feature in the non-collective regime (i.e. large scattering vector) directly measure the free-electron velocity distribution [Gle2003, Lee2009]. In low-temperature highly-degenerate plasmas, as will be produced at FAIR, this gives a direct measure of the free-electron density, and could also be exploited to see the transition of the metal-like free-electron Fermi gas to a non-conducting state, as the density decreases upon target expansion. X-ray scattering experiments require the highest spectrometer efficiencies. Typically highly-oriented graphite crystals (“HOPG”) have been employed, reaching highest integrated reflectivities, at the expense of spectral resolution. More recently, promising results have been obtained with a highly-annealed form of graphite (“HAPG”) [Zas2013], showing a good compromise between resolution and reflectivity.

Given the enormous diagnostic potential of x-ray spectroscopy we regard it crucial to provide a basic set of x-ray crystals for plasma physics experiments at FAIR.

Figure 13: Proposed setup of the VUV-opacity measurement on ion-beam heated foils.

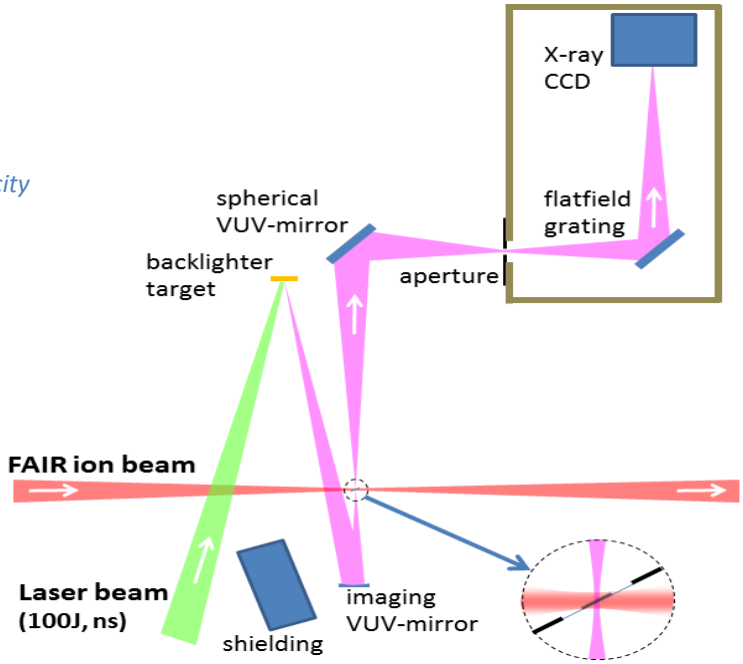

Spectroscopy in the vacuum-ultraviolet (VUV) to soft x-ray spectral region has been proposed to test electronic structure and opacity calculations of dense high-Z elements [Tau2009]. A long-pulse laser driven high-Z plasma emits quasi-continuous VUV radiation and the transmission through the target is spectrally resolved by a blazed flat-field gold grating and detected by an x-ray CCD camera. First proof-of-principle measurements with several 10^9 uranium ions per pulse have shown the viability of the approach. However, heavy-ion generated secondary radiation was found to produce a significant background, which could however be mitigated by aperturing the spectrometer view. To enable measurements using the significantly higher intensity (>10x) ion pulses at FAIR, transport and shaping of the probe radiation by XUV mirrors will be employed. For wavelengths larger than 40nm coatings are available with >30% reflectivity even at normal incidence. Such mirrors can be used to produce an intermediate focus of the radiation transmitted by the target. At this intermediate focus, a much smaller aperture can be placed, and the entire spectrometer behind this aperture enclosed in a separate housing, which will significantly reduce the secondary radiation background (see schematic setup Figure 13). An additional benefit of employing a refocusing mirror is that in the non-spectral direction spatial imaging with resolution <100µm can be achieved. This scheme was recently successfully tested at the PHELIX laser.

Using laser-produced plasmas for backlighting dynamical objects knowledge of the temporal characteristics of the source is of crucial importance. Typical timescales of the hydrodynamic evolution of the heavy-ion heated samples is on the order of some tens of nanoseconds. Therefore, a probe duration below 1 ns is sufficient to avoid temporal smearing of data. For the temporal characterization of backlighting source duration, an array of fast diodes equipped with interference optical and VUV-mirrors and/or selective filters can be used in a tunable regime for temporal characterization of a source in optical, VUV up to Hard X-ray photon energy regions [Bak2001].

3. Particle diagnostics

Particle detectors have been developed for smaller facilities and different beam parameters. We intend to rely on these initial results and develop a detector system based on the following concept: a fast, radiation hard scintillating material coupled to an optical system and a fast-gated, electronic readout system providing temporal resolution.

New fast, gated cameras have been recently put on the market and we intend to test them for their applicability. For the material to convert the particle beam into optical information we intend to explore different scintillating materials, doped fibre arrays and also doped multi-channel plate detectors. Special care will be taken on the response to the unavoidable EMP and hard x-ray background present during most of the foreseen experiments. Also in addition to larger scale detectors we intend to look into closely coupled detectors that can be assembled close to the target for higher detection efficiency.

Proton radiography

In the end of 1990's, Los Alamos National Laboratory (LANL) has developed the technique of high energy proton radiography as a flash radiography system for the study of dynamic systems. 800 MeV protons from a linac have been used at LANL. These studies have focused on measuring fundamental material properties (equation of state, strength, phase transitions...) as well as the physical processes important in predicting the hydrodynamic flow of these materials at high velocity pressure and density (instabilities such as Richtmyer-Meshkov, Rayleigh-Taylor and Kelvin-Helmholtz).

Setups for high energy proton radiography have been also developed at the Institute for Theoretical and Experimental Physics (ITEP) in Moscow, Russia and at the Institute for High Energy Physics (IHEP) in Protvino, Russia, using high energy (800 MeV and 50 GeV at ITEP and at IHEP, respectively) proton beams from synchrotrons. The technique used to form and collect the proton radiographs are very similar.

Many of the fundamental HEDP and WDM experiments require a radiographic system with high spatial resolution - high energy proton microscopy (HEPM). HEPM systems with permanent magnetic quadrupoles have been developed and used in experiments at LANL (pRad, 800 MeV), ITEP (PUMA, 800 MeV) and GSI (PRIOR, 4.5 GeV). The multi-time, high-resolution capability of proton microscopy, as it has been applied to the study of material strength at high strain-rate, is a good example of the unique capability that proton microscopy provides for the study of dynamic materials science.

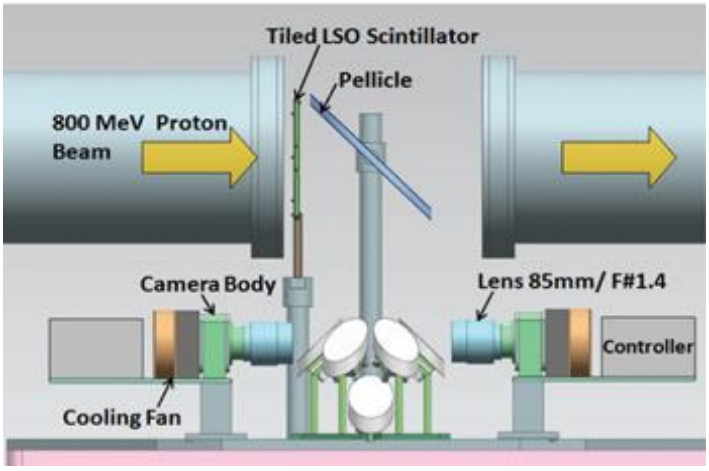

Figure 14: The detector system for the proton- radiography setup pRad (LANL)

High-resolution fast proton detector is a prerequisite for the 3 - 10 GeV proton microscope PRIOR planned at FAIR. Proton flux is converted to visible light by a fast thin scintillation screen. The scintillation light is then imaged by several fast gated high-resolution CCD or CMOS cameras. Figure 14 shows an example of such a detector system employed at the proton radiography setup pRad at LANL, where several individual cameras provide multi-framing capability.

Neutron detection

Fast neutron imaging

Imaging with fast neutrons can be a powerful tool to look into the matter complementary to x-rays or protons. As neutrons only weakly interact with the material and have an inverse Z-dependence of absorption, a low Z material can be detected behind a high Z shielding.

For the neutron imaging system the starting design is based on the neutron imager designed for the National Ignition Facility and successfully used by the consortium at the LANL Trident short pulse laser facility. The three basic functions of the neutron imaging system are conversion of neutron fluence to light, the time gating of neutron fluence based on arrival time of the neutrons at the detector, and the digitization of the optical fluence. The system consists of a coherent array of scintillating fibers, followed by a micro channel plate image intensifier for gating and gain, a series of coherent fiber optic elements for relay and image reduction and a charge-coupled-device (CCD) camera for digitization and recording (Figure 15).

The coherent array of scintillating fibers is a round shaped close pack with a diameter of 80 mm. Each fiber in the array is 5 cm long and 500 µm in diameter. The scintillating material is BCF-20. It converts the neutron fluence to light predominantly via (n, p) and (n, C) reactions with its peak spectral emission is at 492 nm and emitting ≈ 8000 photons per MeV of energy de- posited by ionizing radiation, consisting of neutrons and gamma rays for these experiments. The core material is Polystyrene with refractive index of 1.60. Cladding material is acrylic wit refractive index of 1.49 and thickness of 3% of the fiber diameter. Therefore, the numerical aperture of the fiber is 0.58 and the light trapping efficiency is ~3.5%. During the experiments, the front of the scintillator is covered by an aluminized mylar pellicle to reflect light. This increased the effective trapping by almost a factor of two. The scintillator bundle is manufactured by St. Gobain, formerly known as Bicron. Following the scintillator bundle is a 2:1 imaging fiber optic reducer made by Incom reduces the optical output of the scintillator to 40 mm. A 40 mm micro-channel-plate-image-intensifier (MCPII) produced by Photek provides both an electronic shutter and gain. The MCPII has a S20 photo-cathode, a single micro-channel-plate, and a P43 phosphor. A

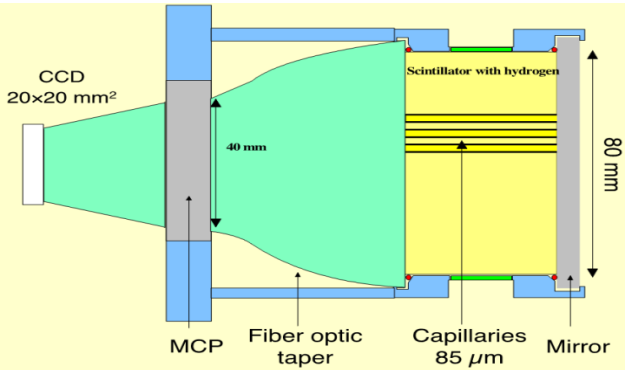

Figure 15: Neutron imaging system as used at the NIF and the LANL trident laser.

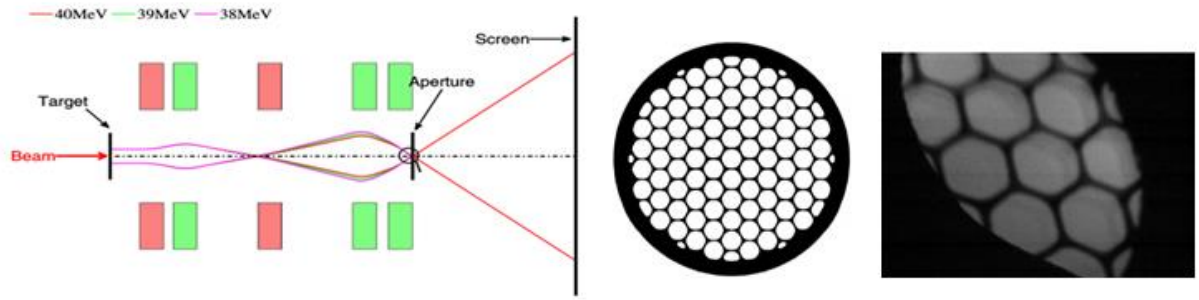

Figure 16: Image of the TEM hexagonal grid by 40 MeV electron beam (Y. Zhao, private communication).

second 5:3 Incom imaging fiber optic reducer allows coupling of the MCPII to a three foot long coherent fiber optic rope. This rope is made by Schott and allows a camera to record the image outside of the direct neutron beam line-of-sight. The camera used is a Spectral Instruments SI-800 camera with a 2k by 2k e2v scientific grade back-thinned CCD with 13.5 µm pixels.

Secondary neutrons and lower energy neutrons.

The use of moderated, thermal neutrons is of high interest as this might be a unique opportunity to measure temperatures inside a sample. Today's high efficiency detectors, based mostly on He3, become limited in availability and cost. We are looking into a novel scheme of detectors based on doped micro-channel plates and a fast readout system that has recently be patented by one of our industry partners. Such detectors are only useful if they can be used in pulsed energy environments, like ion beam impact or laser driven sources. Therefore we plan to test and develop those detectors to be used in APPA experiments. The 40mm MCP detector is doped with ^{10}B or Gd and incorporated in either base glass melting or as a thin film internal coating. It is usually coupled to a Medipix-2 digital readout system, however, the more recent Medipix-3 could be an interesting option. It is expected to yield a 50 µm spatial resolution with a thermal neutron sensitivity of great 40% and a gamma sensitivity of less than 1%. Usually it is equipped with a P46 (fast green) or P47 (fast blue) readout screen.

Electron beams for direct and indirect target imaging

Electron beams have a great potential for applications in HED experiments. Relativistic electrons can be used directly for imaging applications, or for production of spatially coherent, highly brilliant x-ray and gamma-ray sources as well as high energy bremsstrahlung.

One of the first applications for imaging of solid targets with high spatial and temporal resolution was currently demonstrated by the group of Tsinghua University, China. The 40 MeV electron beam from the eRAD-electron accelerator was used to radiograph Transmission Electron Microscope hexagonal grid. The magnetic telescope with 7-fold magnification of the target on the detector has ensured 5-10 µm spatial resolution. Imaging was made with one electron bunch of 1 ps time duration.

The possibilities of the electron acceleration by lasers have been demonstrated numerically and experimentally on PW and TW laser systems [Will2013, Gray 2012, Mao2012, Tonch2013]. Results of 3D Particle-in-Cell simulations of the electron beam energy spectrum generated in the case of oblique incident PHELIX-laser pulse 1w, 150J, 500 fs) on a Cu massive target, accounting for different pre-plasma

scales and laser beam polarization are presented in Figure 17. For available PHELIX-laser parameters simulation promises nC electron bunch of low divergence, up to 150 MeV energy and ps time duration.

Laser accelerated electron bunches can be used for creation of highly brilliant coherent x-ray and gamma-ray sources. In under-dense plasma, the laser field acceleration leads to generation of electrons up to GeV energies [Mal2002, Kne2006, Ton2013]. During the longitudinal acceleration process electrons undergo also transversal oscillations in the plasma channel due to the Lorenz force of the laser field. This radiation is strongly directed and spatially coherent, maximum of the spectrum can be tuned by laser and target parameters. Micrometer source sizes have been deduced from experiments [Sch2012].

The Compton scattering (also known as Thomson backscattering for low energy limit $h\nu >> 0.5$ MeV) of a photon beam on the laser accelerated electron beam has been recently demonstrated to generate a broadband spectrum of x-rays extending to hundreds of keV [Phu2012].

Given these outstanding recent achievements and progress we intend to follow the current development of sources based on laser-accelerated electrons, to build up some expertise in this field which will help us evaluate the diagnostic potential of such sources for applications at FAIR. For this work some basic detector options will have to be available. For the spectral analyses of the x-ray and gamma secondary sources Hard X-ray Detectors (HRD) based on the Lambert-Beer law will be used for the photon energies below 1 MeV, where a photo absorption mechanism of the signal attenuation is playing a major role. Methods of the material nuclear activation will be applied up 10 MeV photon energy and analyses of the Compton scattered photons and electrons will be performed in the intermediate photon energy region between 1 and 10MeV.

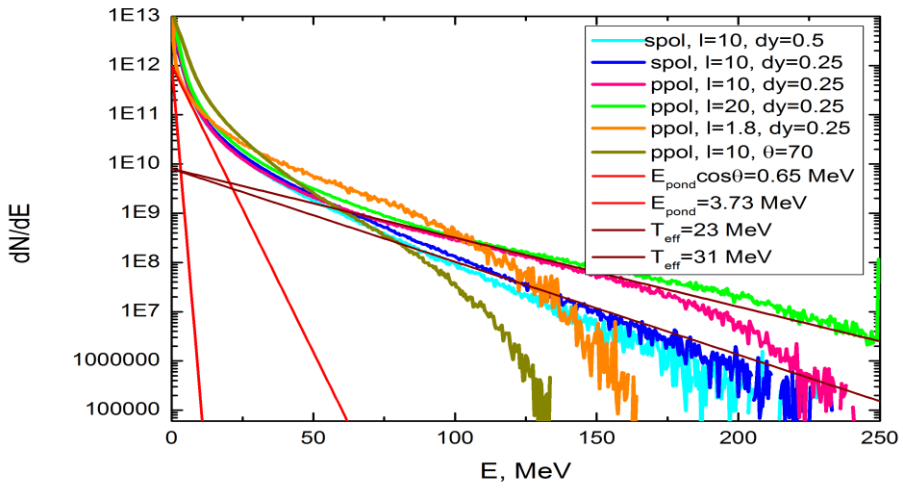

Figure 17: 3D PIC-simulations of laser accelerated electron beam resulted from interaction of the oblique incident 500fs PHELIX-laser pulse with a massive Cu-target (N. Andreev et al., JIHT Moscow, priv. comm.)

Experiment preparation lab equipment

On the floor above the APPA experimental cave approx. 35m^2 of lab space has been reserved. This room will serve as a preparation and setup lab where diagnostic setups can be assembled, pre-aligned and tested. For these purposes, a copy of the beam interaction chamber will be located in this room. The lab will also be used to perform initial performance qualification of detection systems (framing and streak cameras), as well as regular calibration tasks. In addition, laser pulses from the 100J long-pulse laser system can be directed to this room, allowing e.g. to characterize laser-driven backlighting sources and schemes or qualify the VISAR setup.

Some initial equipment and infrastructure should be provided initially. This includes two optical tables, a basic set of optomechanics and optics and an additional small vacuum chamber. In addition, XUV- and x-ray testing facilities will be provided.

Optical setup equipment

Here we foresee an initial set of 1" and 2" mounts (lenses, mirrors), the respective posts and mounting brackets, and manual translation stages, as well as a set of 1" and 2" mirrors, a range of lenses, and alignment cameras. For focusing the 100J laser pulses into the vacuum chamber (see following paragraph), 4" vacuum window and focusing lenses will be available. Optical arrangements will be setup on two optical tables (e.g. 3m x 1.5m).

Vacuum interaction chamber

In order to enable testing of diagnostic setups for the main target chamber in the APPA-cave, a replica of a part of the target chamber will be built. It consists of the "beam interaction" section of the main target chamber, which is centered around the main interaction point with ports that directly view the target location (approx. dimensions: 1.2m x 1.5m x 1m height x width x length). This chamber will be located in the experiment preparation lab and is provided to the experimental teams to allow set up, alignment and validation of diagnostics setups before fielding the instruments in the actual experiment inside the APPA cave.

Vacuum environment is also necessary for testing of VUV and soft X-ray-components and setups, and when focusing the 100J long-pulse laser onto a target, e.g. for characterization and optimization of laser-driven x-ray backlighter sources such as He-alpha sources in the keV range, or broadband thermal sources. To allow this type of activities independently of direct preparations for upcoming beamtimes we foresee an additional small vacuum chamber in the experiment preparation lab. For these applications a vacuum vessel with a diameter of no more than 1m at a height of <0.5 m should be sufficient. Convenient access for setting up will be through the top lid, which at this size can be opened without use of a crane (e.g. by gas cylinder springs). Several standard (ISO-K or CF, to be determined) flanges of 4" diameter will be distributed around the chamber for injecting and extracting laser beams or diagnostic views. A mechanically isolated breadboard inside the chamber will allow stable setups with stable alignment even upon pump-down. The height of this breadboard will be approximately the same as that of the optical tables, to allow easy injection and extraction of beams. Pumping of the vacuum chamber is by standard oil-free roughing pump and small turbo pump station. Figure 18 shows a possible arrangement of the setup lab.

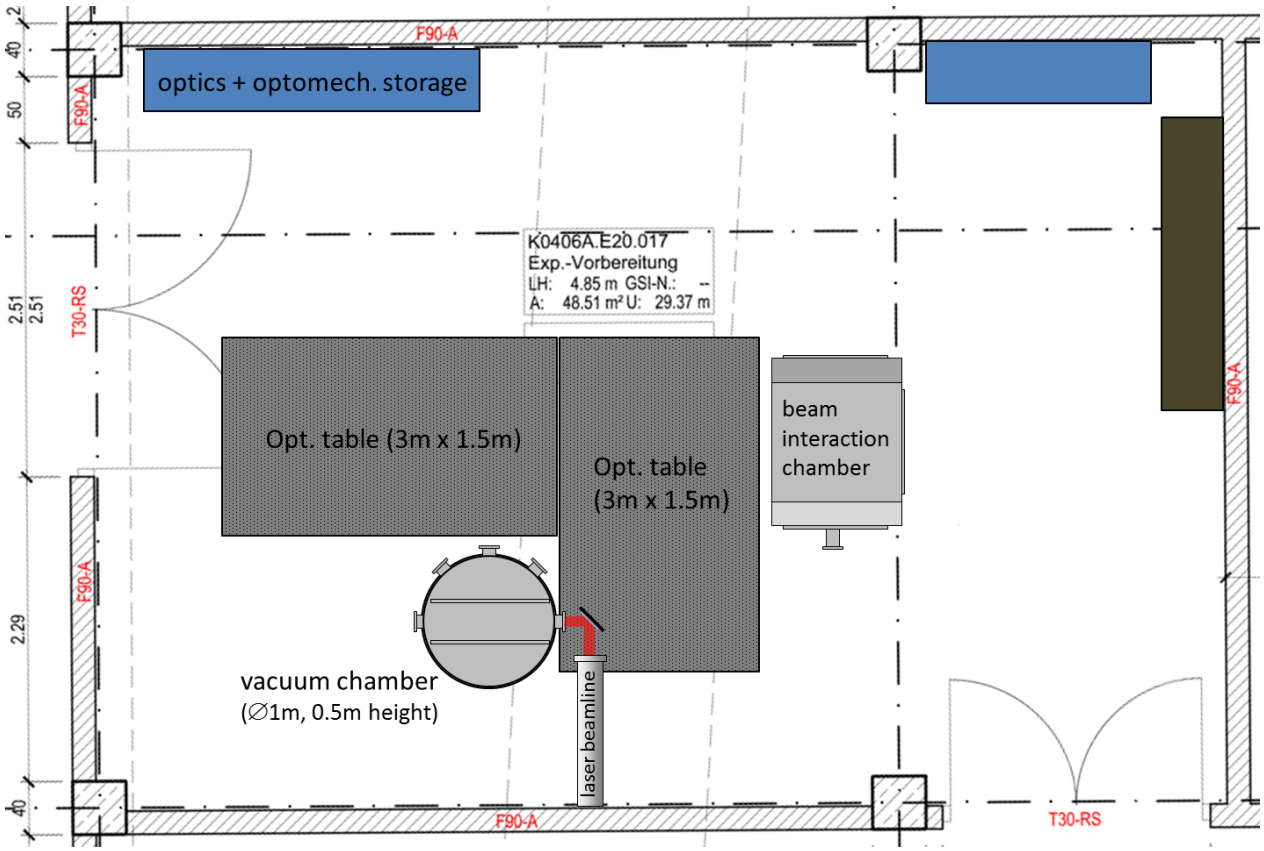

Figure 18: Possible arrangement of the Experiment Preparation Lab.

X-ray diagnostics testing, characterization & calibration

Given the large effort and expenses to field experiments, as well as limited target area access due to radiation safety precautions, accurate knowledge of detector performance is mandatory. Degradation of the crystal reflectivity is likely to occur, due to aging as a consequence of the high load of radiation exposure. Grating diffraction efficiencies into different diffraction orders in the XUV are mostly unknown. Filter transmissions can be calculated, but might differ significantly e.g. due to oxidation and/or unknown density by implementation of an evaporation technique. Spectral and spatial resolution depends on the crystal quality and the alignment accuracy. Also, new detector developments, such as the scintillator based imager, require testing to assess performance and improve characteristics.

We therefore foresee dedicated testing equipment to enable accurate characterization and calibration of x-ray diagnostic components. These consist in a high-power (>1kW) x-ray tube with exchangeable anode, as well as a discharge XUV source. The latter will be operated at vacuum conditions. Two monochromators (crystal for x-ray, grating-based for XUV) will be provided for monochromatic testing. A CdTe-diode x-ray detector will allow absolute measurements of the x-ray tube emission spectrum, and calibrated XUV-diodes will be used for the XUV source monitoring. A set of motorized stages, e.g. for rocking curve measurements, or surface morphology should be available. For absolute detector calibration (CCD-cameras, image plates, scintillators etc.) and quantum efficiency measurements a set of radioactive sources covering the broad region of photon energies from some of keVs (Fe56) up to 1 MeV (Co60) will be used.

References

[Bak2001] Yu. Bakshaev et al., Rev. Scient. Instr. 72, N1(2001)1210-1213

[Ben2008] A. Benuzzi-Mounaix et al., Phys.Rev. E 77, 045402 (2008)

[Ben2011] A. Benuzzi-Mounaix et al., PRL 107, 165006 (2011)

[Cel2004] P. M. Celliers et al., Rev. Scient. Instr. 75, 4916 (2004)

[Coc1979] C. L. Cocke, Phys. Rev. A 20, 749 (1979).

[Cow2004] T. Cowan et al., Phys. Rev. Lett. 92, 204801 (2004)

[Fae1994] A.Ya. Faenov et al., Phys. Scr. 50 (1994) 333

[Gle2003] S. H. Glenzer et al., Phys. Rev. Lett. 90, 175002 (2003)

[Gray2011] R.J. Gray et al., Appl. Phys. Lett 99, 171502 (2011)

[HED2005] Technical Proposal for Design, Construction, Commissionning and Operation of the HEDgeHOB, January 14, 2005

[Kne2006] S. Kneip et al., Phys. Rev. Lett 96 (21)2006

[Knu2008] M.D. Knudson, et al., Science 322, 1822 (2008)

[Koz2003] A. Kozyreva et al., Phys. Rev. E 68, 056406 (2003)

[Kri2008] A. L. Kritcher et al., Science 322, 69 (2008)

[Lee2009] H. J. Lee et al., Phys. Rev. Lett. 102, 115001 (2009)

[Lor2011] W. Lorenzen et al., Phys. Rev. B 84, 235109 (2011)

[Mal2002] V. Malka et al., Science 298(5598) (2002)1596-1600

[Man2010] A. Mancic et al., PRL 104, 035002 (2010)

[Mao2012] J.Y. Mao et al., Phys Rev. E 85(2012)025401

[Maz2014] S. Mazevet et al., Phys. Rev. B 89, 100103 (2014)

[Net2008] N. Nettelmann et al., Astrophys. Journ. 683, 1217 (2008)

[Ros2002] O. Rosmej et al., Nuc. Instr. and Meth. A 495 (2002) 29–39

[Par2008] H.-S. Park et al., Phys. Plasmas 15, 072705 (2008)

[Pel2010] A. Pelka et al., PRL 105, 265701 (2010)

[Phu2012] K.Ta. Phuoc et al., Nature Photonics 6(5)(2012)308-311

[PRI2009] PRIOR Technical Design Report, GSI, May 2009

[Rec2009] V. Recoules et al., Phys. Rev. B 80, 064110 (2009)

[Rot2013] M. Roth et al., Phys. Rev. Lett. 110, 044802 (2013)

[Saw2009] H. Sawada et al., Phys. Plasmas 16, 052702 (2009)

[Sch2012] M. Schell et al., Phys. Rev. Lett 108(7) 2012

[See2012] J. Seely et al., Rev. Scient. Instr. 83, 10E112 (2012)

[Tah2005] N. A. Tahir et al., Phys. Rev. Lett. 95, 035001 (2005)

[Tah2010] N. A. Tahir et al., N. Journ. Phys. 12, 073022 (2010)

[Tah2011] N. A. Tahir et al., Phys. Plasmas 18, 032704 (2011)

[Tah2014] N. A. Tahir, private communication

[Tau2009] An. Tauschwitz et al., Appl. Phys. B 95, 13 (2009)

[Tom2011] R. Tommasini et al., Phys. Plasmas 18, 056309 (2011)

[Ton2013] T. Tonchian, Habilitation thesis, Heinrich-Heine-Universität Düsseldorf, 2013

[Ulr2012] A. Ulrich, Laser and Particle Beams 30, 199-205 (2012)

[Var2009] D. Varentsov et al., Contrib. Plasma Phys. 48 586-594

[Vin2009] S. M. Vinko et al., High En. Dens. Phys. 5, 124 (2009)

[WDM2006] WDM—radiative properties of warm dense matter produced by intense heavy ion beams. FAIR Baseline Technical Report, vol. 5, 2006 (paragraph 5.3). Available at http://www.gsi.de/fair/reports/btr.html

[Wil2013] H. F. Wilson et al., Phys. Rev. Lett. 110, 151102 (2013)

[Will2013] L. Willingale et al., N. Journ. Phys. 15, 025023 (2013)

[Zas2013] U. Zastrau et al., Journ. Instr. 8, P10006 (2013)